



Molecular Model of the G Protein α Subunit Based on the Crystal Structure of the HRAS Protein

Stephen R. Holbrook, Sung-Hou Kim

Proceedings of the National Academy of Sciences of the United States of America,
Volume 86, Issue 6 (Mar. 15, 1989), 1751-1755.

Your use of the JSTOR archive indicates your acceptance of JSTOR's Terms and Conditions of Use, available at <http://www.jstor.org/about/terms.html>. JSTOR's Terms and Conditions of Use provides, in part, that unless you have obtained prior permission, you may not download an entire issue of a journal or multiple copies of articles, and you may use content in the JSTOR archive only for your personal, non-commercial use.

Each copy of any part of a JSTOR transmission must contain the same copyright notice that appears on the screen or printed page of such transmission.

Proceedings of the National Academy of Sciences of the United States of America is published by National Academy of Sciences. Please contact the publisher for further permissions regarding the use of this work. Publisher contact information may be obtained at <http://www.jstor.org/journals/nas.html>.

Proceedings of the National Academy of Sciences of the United States of America
©1989 National Academy of Sciences

JSTOR and the JSTOR logo are trademarks of JSTOR, and are Registered in the U.S. Patent and Trademark Office. For more information on JSTOR contact jstor-info@umich.edu.

©2001 JSTOR

Molecular model of the G protein α subunit based on the crystal structure of the HRAS protein

(signal transduction/homology modeling/sequence alignment)

STEPHEN R. HOLBROOK AND SUNG-HOU KIM

Division of Chemical Biodynamics, Lawrence Berkeley Laboratory, and Department of Chemistry, University of California, Berkeley, CA 94720

Communicated by Melvin Calvin, October 10, 1988

ABSTRACT A structural model of guanine nucleotide-binding regulatory protein α subunits (G_α subunits) is proposed based on the crystal structure of the catalytic domain of the human HRAS protein ($p21^{ras}$). Because of low overall sequence similarity, structural and functional constraints were used to align the G_α consensus sequence with that of $p21^{ras}$. The resulting G_α model specifies the spatial relationship among the guanine nucleotide-binding site, the binding site of the $\beta\gamma$ subunit complex, likely regions of effector and receptor interaction, and sites of cholera and pertussis toxin modification. The locations in the model of the experimentally determined sites of proteolytic digestion, point mutation, monoclonal antibody binding, and toxin modification are consistent with and help explain the observed biological activity. Two important findings from our model are (i) the orientation of the G_α model with respect to the membrane and (ii) the identification of the spatial proximity of the N- and C-terminal regions. Furthermore, by analogy to $p21^{ras}$, the model assigns specific residues in G_α required for binding the guanosine (G-box) and phosphates (PO₄-box) and identifies residues potentially involved in the conformational switch mechanism (S-box). Specification of these critical regions in the G_α model suggests guidelines for construction of mutants and chimeric proteins to experimentally test structural and functional hypotheses.

The three-dimensional structure of the GDP-bound catalytic fragment of the human HRAS protein (1) $p21^{ras}$ provides a basis for predicting structural models of other GDP/GTP binding proteins or subunits. A particularly interesting example of this class is the α subunit (G_α) of the guanine nucleotide-binding regulatory protein (G protein) family.

G proteins constitute a family of signal transducers (2–5) that relay an extracellular signal received by a transmembrane receptor protein to a membrane-bound effector protein. They perform this transduction by switching between a “signal-on” activating conformation and a “signal-off” latent conformation depending on whether they are bound by GTP or GDP, respectively. The G proteins consist of three subunits denoted G_α , G_β , and G_γ . The G_β and G_γ form a tight functional complex that may help anchor G proteins to the membrane. G_α is thought to provide G proteins with their specificity for particular receptors and effectors and, as the site of guanine-nucleotide binding and GTP hydrolysis, contains the conformational switch mechanism by which G proteins become activated. Currently, the best characterized mammalian G proteins are the G_s and G_i proteins, which stimulate and inhibit adenylyl cyclase, respectively, the transducins (G_{t1} and G_{t2}) of the visual rod and cone systems, and the G_o protein found in large quantities in brain tissue (3).

Three models of the three-dimensional structure of G_α have been proposed (6–8) based on the x-ray crystal structure of

the guanine nucleotide-binding domain of the bacterial elongation factor Tu (G-EF-Tu) (9, 10). Although these models have been useful in interpreting experimental data and formulating and testing hypotheses of G-protein function, we feel that a model based on the structure of $p21^{ras}$ is superior for several reasons. (i) The sequences of the G_α chains are more similar overall to that of $p21^{ras}$ than G-EF-Tu, especially in regions involved in phosphate binding and GTPase activity (11). Specifically, in our alignment 22% of all residues and 44% of those in the phosphate-binding region of $p21^{ras}$ are identical to G_α residues, versus 16% and 28% in the alignment of G-EF-Tu with G_α (6). (ii) In the crystal of G-EF-Tu the N-terminal half of the protein has been trypsin modified so that 15 residues are removed. This region corresponds to an area of $p21^{ras}$ implicated in effector interaction. (iii) The structure of $p21^{ras}$ has been refined at 2.2 Å (12), resulting in more accurate atomic coordinates and better definition of secondary structure. (iv) The biological role of $p21^{ras}$ as a membrane-bound protein and putative regulator of cellular proliferation and differentiation (13) is more closely related to that of the G protein family.

Of the available sequences of G_α subunits, $G_{\alpha s}$ differs most from the others and, therefore, was not used in our analysis. The remaining five G_α sequences, $G_{\alpha i1}$, $G_{\alpha i2}$, $G_{\alpha o}$, $G_{\alpha t1}$, and $G_{\alpha t2}$ (14–16), were used to determine a G_α consensus sequence that was subsequently aligned to the sequence of $p21^{ras}$. By assuming aligned regions have the same three-dimensional structure, a model for the nucleotide-binding domain of G_α was constructed.

METHODS

Sequence Alignment. Even distantly related proteins that share a common function are expected to conserve the amino acids and three-dimensional fold required for that function, although they may show little overall sequence similarity. We, therefore, used the regions in $p21^{ras}$ known to be required for structure and function to direct alignment of $p21^{ras}$ with G_α . The primary features of $p21^{ras}$ examined in this context were (i) subsequences or residues involved in substrate or ligand binding or catalysis, (ii) helical, sheet, turn, and loop structures, (iii) hydrophobic or buried (nonaccessible) residues, and (iv) mutations affecting biological function. The residue numbers of the structural and functional elements used to guide the alignment are given in Table 1.

A modified version of the computer program MALIGN (17) was used for all sequence alignment. This program identifies consecutive runs of homologous residues (regions) common to the sequences being aligned. These regions are then aligned and gaps are introduced to maximize matches. We have modified this program to allow for variable gap penalties and weights for sequence matching depending on sequence position. Regions known to be functionally or structurally

The publication costs of this article were defrayed in part by page charge payment. This article must therefore be hereby marked “advertisement” in accordance with 18 U.S.C. §1734 solely to indicate this fact.

Abbreviations: G protein, guanine nucleotide-binding regulatory protein; G_α , G protein α subunit; G-EF-Tu, guanine nucleotide-binding domain of the bacterial elongation factor Tu.

Table 1. Residues of the HRAS catalytic domain used to constrain sequence alignment

Structure-function constraint	p21 ^{ras} residue numbers
α -Helices	17-26, 87-105, 127-137, and 151-171
β -Strands	1-7, 40-44, 54-59, 77-82, 110-117, and 140-144
Phosphate-binding loop	12-17
Ribose binding	30 and 117
Guanine binding	28, 116, 119, 145, and 146
Transforming mutations	12, 13, 15, 16, 59, 61, 63, 116, and 119
Buried residues, hydrophobic	77-84 and 111-116

important were weighted highly in the alignment, thereby favoring alignment of these p21^{ras} sequences with corresponding sequences in G α . Gap penalties were increased (by up to 8 times) within regions of secondary structure so as to discourage internal insertions or deletions.

For the highly homologous G α proteins, we required amino acids be identical in alignment. However, in aligning the G α consensus sequence with p21^{ras}, we categorized the amino acids by hydrophobicity as indicated in the legend to Fig. 2 and searched for patterns of these classes. The pattern of hydrophobic-hydrophilic residues in proteins is related to their three-dimensional structure in at least two aspects, (i) hydrophobic residues tend to be buried in the interior of proteins and hydrophilic residues are generally found on the surface of the protein exposed to solvent (18), and, as a

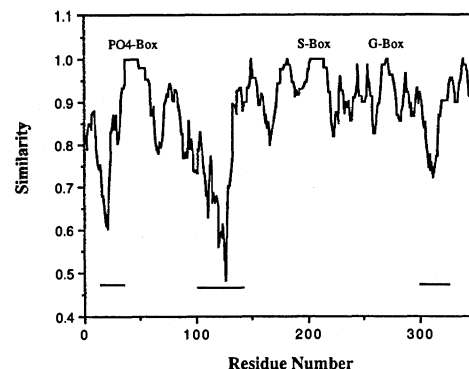


FIG. 1. Similarity plot for five aligned G α subunit sequences. The sequence numbers correspond to the G α consensus sequence. Similarity scores are based on the matrix of Feng *et al.* (20) and smoothed by averaging over a window of seven amino acids. Regions of similarity score 1.0 are identical. Lower scores reflect greater differences in amino acid type. The highly conserved PO₄-box, S-box, and G-box are indicated. The variable regions residues 11-23, residues 97-132, and residues 307-316 (similarity <0.8) are highlighted by underlines.

corollary, (ii) α -helices and β -strands exhibit characteristic periodicities of hydrophobic residues to form the amphipathic surfaces necessary for making favorable contacts both within the protein and with the solvent (19).

Sequence Similarity Comparison. To quantitate agreement among aligned G α sequences, the average similarity, as

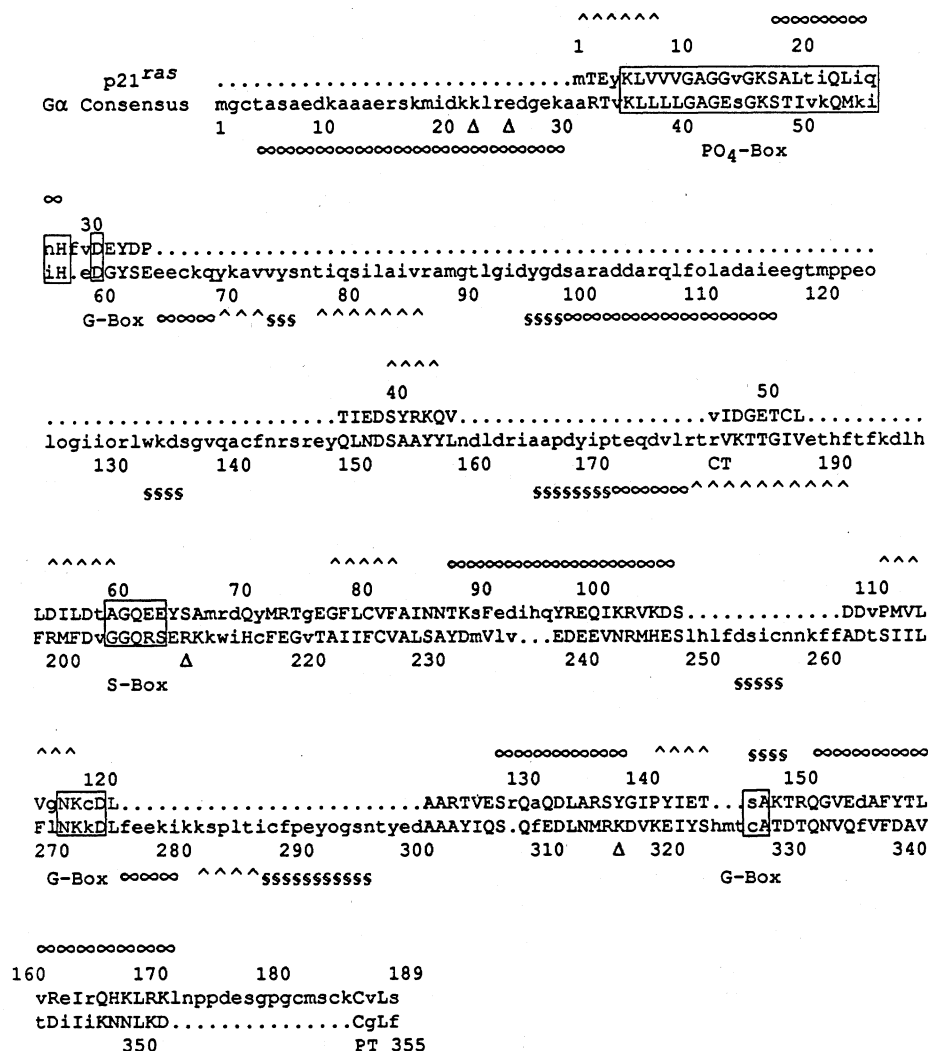


FIG. 2. Alignment of p21^{ras} and G α consensus sequences. G α consensus was obtained by multiple sequence alignment as described in the text and represents the most frequently occurring amino acids among the sequences used as a data base. The letters o in G α consensus are at sites where all five subunit sequences contain a different amino acid. The alphabet used for alignment of p21^{ras} and G α consensus was as follows: hydrophilic, A, D, E, G, H, K, N, P, Q, R, S, T, Y; hydrophobic, C, F, I, L, M, V, W, according to the scale of Rose *et al.* (18). A total of 74% (139/189 residues) of the residues of p21^{ras} are aligned with homologous (in hydrophobic alphabet) residues in G α consensus and are indicated by capital letters, whereas residues differing in hydrophobic alphabet are denoted by lowercase letters. Of the aligned residues 22% (41/189 residues) are identical. The secondary structure of p21^{ras} observed in the crystal structure of its catalytic domain (residues 1-171) is indicated above the p21^{ras} sequence: ∞ , α -helix; \wedge , β -strand; \S , turn. The predicted secondary structure for nonhomologous regions of G α is indicated below the consensus sequence. Residues comprising the PO₄-box, the S-box, and the G-box are enclosed by boxes and labeled. Trypsin cleavage sites are indicated by arrowheads, and the ribosylation targets of cholera and pertussis toxins are denoted by CT and PT, respectively.

judged by an amino acid similarity matrix (20), between all combinations of amino acids occurring at a particular position in the sequence was computed. These scores were then smoothed by calculating a running average in a window around each position. The resulting plot of sequence similarity versus residue number is shown in Fig. 1.

Secondary Structure Prediction. A modification of the Chou-Fasman approach (21) was made to utilize information contained in the diversity of the aligned G_α sequences in predicting a consensus secondary structure. In this procedure, average, minimum, and maximum probabilities of helix, turn, or sheet were calculated from the Chou-Fasman parameters corresponding to the various amino acids appearing at a given position and then smoothed by averaging over several residues. This approach is based on the assumption that homologous sequences assume the same secondary structure. For example, a proline appearing in any one sequence would strongly argue against a helical structure, predicted by the minimum of helical probabilities at that position.

RESULTS AND DISCUSSION

Multiple sequence alignment of five G_α subunits ($G_{\alpha 1}$, $G_{\alpha 2}$, $G_{\alpha o}$, $G_{\alpha t1}$, and $G_{\alpha t2}$) required introduction of only five gaps, four of just one residue (position 123 in $G_{\alpha 1}$, position 129 in $G_{\alpha t1}$ and $G_{\alpha t2}$, and position 313 in $G_{\alpha o}$), and one of four residues (positions 18–21 of $G_{\alpha t2}$). The length of the G_α consensus sequence is the same as that of $G_{\alpha 2}$ since no insertions or gaps were introduced. This alignment is very similar, although not identical, to previous alignments (3, 6) and is available from the authors on request. Although the G_α sequences are clearly very similar overall, certain regions are quite variable as shown in Fig. 1. A total of 52% of the aligned residues are identical in all subunit sequences, with only five positions having a different residue present in each sequence. The consensus sequence, representing the amino acids occurring most frequently among the aligned sequences, was used in the subsequent alignment with $p21^{ras}$.

In aligning the $p21^{ras}$ sequence with the G_α consensus sequence, matches were weighted according to the degree of conservation of the amino acids in the G_α alignment. Also, high weights were used to force alignment of two regions of $p21^{ras}$ known to be involved in GDP binding, as well as a region containing sites of transforming mutations (see Table 1), with regions of G_α consensus shown to be very similar by subsearches. Gap penalties were adjusted to favor insertion outside regions of $p21^{ras}$ secondary structure (i.e., loops) (22, 23). The resulting alignment of $p21^{ras}$ (residues 1–189) and the G_α consensus sequence (residues 1–355) is given in Fig. 2. Because of the generally low sequence homology between $p21^{ras}$ and G_α , alternative alignments are clearly possible, but structural information available from $p21^{ras}$ together with the secondary structure prediction of G_α best agree with the alignment presented here. This alignment differs significantly from those presented previously (3, 6). The aligned residues are proposed to share a common secondary and tertiary structure with $p21^{ras}$ as illustrated schematically in Fig. 3. The predicted secondary structure of regions of G_α not aligned with the $p21^{ras}$ sequence is shown in Fig. 2.

The model of G_α shown in Figs. 2 and 3 can be used to understand and interpret the extensive biochemical and genetic studies on G_α chains summarized in Table 2 and to associate specific regions of the structure with their function in signal transduction.

GDP/GTP Binding Sequences (PO₄-Box and G-Box). The residues involved in GDP binding have been clearly identified in the refined x-ray crystallographic model (12) of $p21^{ras}$. The corresponding residues in G_α (Fig. 2) are postulated to serve the same functions. Specifically, Asn-116 and Asp-119 of

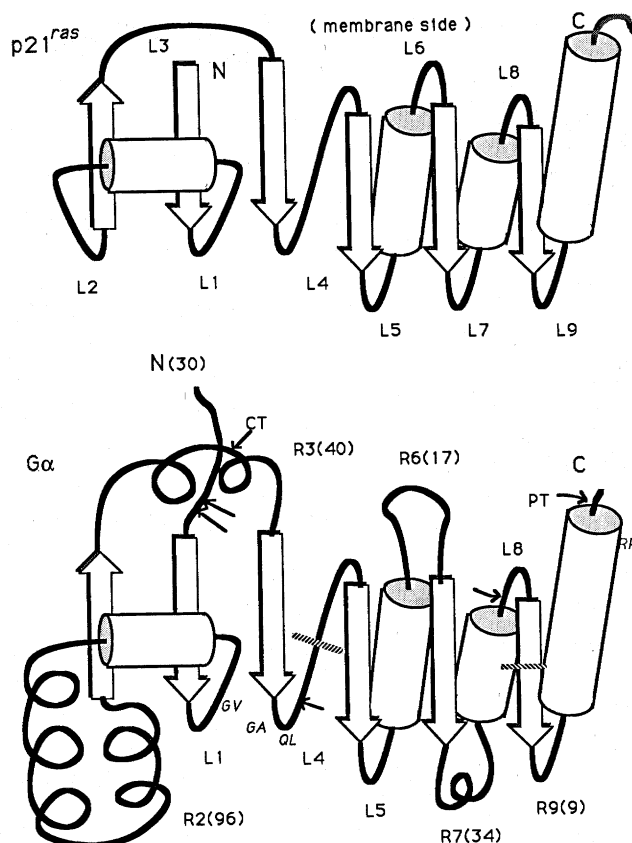


Fig. 3. Schematic (topological) diagrams of the $p21^{ras}$ structure (Upper) and the model of G_α (Lower). β -Strands are indicated by thick arrows, α -helices are indicated by cylinders, and the loop regions are indicated by black lines connecting the secondary structural elements. In three dimensions, the β -sheet is rolled up and twisted in such a way that the N- and C-terminal regions come close together (C_α separation, 9 Å). β -Strands, α -helices, and loops are numbered starting from the N terminus. Areas where relatively short loops in $p21^{ras}$ (L2, L3, L6, L7, and L9) are replaced by longer sequences in G_α are labeled as R2, R3, R6, R7, and R9 and the number of residues is indicated in parentheses. The sites of tryptic cleavage (arrows) and ADP-ribosylation by cholera toxin (CT) and pertussis toxin (PT), are indicated, as well as the point mutations described in Table 2. GV, a Gly \rightarrow Val substitution in the PO₄-box; GA and QL, Gly \rightarrow Ala and Gln \rightarrow Leu substitutions in the S-box; and RP, an Arg \rightarrow Pro substitution near the C terminus. Hatched bars are junction sites for the chimeric proteins described in Table 2.

$p21^{ras}$, which bind the guanine base, are present in all G_α sequences as residues 270 and 273 of the consensus. Asp-30 and Lys-117 of $p21^{ras}$, which bind to the ribose of GDP, have identical counterparts as residues 59 and 271 of G_α consensus. Although the guanine-binding residue Ser-145 of $p21^{ras}$ is not aligned with an identical residue in G_α consensus, its counterpart Cys-326 can form the same type of hydrogen bond to the base. Collectively, these guanosine-binding residues may be referred to as the G-box.

The phosphate-binding loop in $p21^{ras}$ does not interact through amino acid side chains, but instead requires a glycine-rich sequence (residues 10–15 of $p21^{ras}$) to form the appropriate binding pocket. In addition, electrostatic interactions are supplied by Lys-16 and a metal cation bound to Ser-17 of $p21^{ras}$. The corresponding residues in G_α consensus are Gly-40 to Gly-45, Lys-46, and Ser-47. The presence of serine in G_α at the position analogous to Ser-17 in $p21^{ras}$ suggests that a divalent cation is also bound at this site in G_α .

Moller and Amons (11) have identified a phosphate-binding consensus sequence, Gly-(Xaa)₄-Gly-Lys, in mononucleotide-binding proteins. This sequence is part of a larger

Table 2. Genetic and biochemical studies of G_α chains

Type	Consensus location	Implication	G_α chain(s)	Ref(s).
Partial proteolytic digestion				
N-terminal cleavage by trypsin	22	Determines ability to bind $G_{\beta\gamma}$ and N-terminal fragment remains membrane bound	G_t , G_o , G_i	24–26
by <i>Staphylococcus aureus</i> V8	25	Cleavage blocked by $G_{\beta\gamma}$ binding	G_t	27
C-terminal cleavage by trypsin	315	Retains ability to activate effector	G_t , G_o , G_i	24, 25
Internal cleavage by trypsin	209	Only in absence of GTP analogue	G_t , G_o , G_i	24, 25
Mutation				
<i>unc</i> (Arg → Pro)	350	Blocks activation of G_s by receptors	G_s	28
H21a (Gly → Ala)	204	Blocks conformational change due to GTP binding but does not dissociate from $G_{\beta\gamma}$	G_s	29
Phosphate-binding region (Gly → Val)	42	Poorly stimulates adenylyl cyclase (not activating as in p21 ^{ras})	G_s	30
Conserved Gln (Gln → Leu)	205	Constitutively activates adenylyl cyclase even in absence of agonists and may reduce GTPase activity as in p21 ^{ras}	G_s	30
Chimera				
G_{ai}/G_{as}	212	Receptor–effector interaction sites are in the C-terminal 40% of G_s	G_i , G_s	31
G_{at}/G_{as}	212	Receptor–effector interaction sites are in the C-terminal 40% of G_s	G_t , G_s	30
G_{as}/G_{ai}	319	Constitutively activates adenylyl cyclase the effector activating region not past 319	G_s , G_i	*
Monoclonal antibodies				
4A, 7A, 7B, 7C, and 7D	316–328	Binding blocks interaction with receptor	G_t	7
Synthetic peptide				
C-terminal region	316–333	Competes for binding of G_t to receptor	G_t	32
C-terminal fragment	345–355	Competes for binding of G_t to receptor	G_t	32
Toxin				
Pertussis toxin	352	Blocks receptor stimulation and binding	G_i , G_o , G_t	33
Cholera toxin	179	Decreases G_α affinity for $G_{\beta\gamma}$ and reduces GTPase activity	G_s , G_t	34

*G. L. Johnson, personal communication.

β -turn- α structural motif (1) encompassing residues 5–27 in p21^{ras} and corresponding to residues 35–57 of G_α consensus. This sequence is conserved among all G_α subunits (Fig. 1) and designated as the PO₄-box.

The Potential Conformational Switch (S-Box). The residues in p21^{ras} identified as sites of transforming mutations are of two types, those directly interacting with the bound GDP and those in the loop adjacent to the phosphate-binding loop (1). Ala-59, Gln-61, and Glu-63 of p21^{ras} are likely to be involved in binding the γ -phosphate and/or to be involved in the conformational switch proposed to occur on GTP/GDP exchange (12). We refer to this critical switch region as the S-box. The corresponding residues in G_α consensus are Gly-203, Gln-205, and Ser-207. Among G_α subunits, residues 200–217 are completely invariant, implying a significant role for loop L4 (Fig. 3). As seen in Table 2, mutation of Gln-205 → Leu produces a G_s that constitutively activates adenylyl cyclase (30), presumably by locking the structure into a specific activating conformation. Also, mutation of Gly-204 → Ala appears to block conformational change due to GTP or analogue binding, as judged by lack of trypsin digestion and $G_{\beta\gamma}$ dissociation (29). These results implicate this region as a critical component of the conformational switch in G proteins.

Effector Binding Site. The region of highest variability (Fig. 1) within the G_α proteins occurs between residues 57 and 152. This region corresponds to replacement of the short loop 27–39 of p21^{ras} (L2, Fig. 2) with a much longer domain (R2) in the G_α proteins. This loop has been proposed as the effector-binding region in RAS proteins (35) and more recently as the region thought to bind the GTPase-activating protein (GAP

(36, 37). Analogy to p21^{ras} suggests this highly variable region of G_α to be its effector-binding domain. The size of this domain means that it may spatially interact with virtually any other region of G_α .

Available experimental data (Table 2), however, suggest that effector interaction occurs somewhere between residues 212 and 315 of the G_α consensus sequence. Residues 248–260 or residues 275–299 are the most likely candidates for this function. Both sequences (R6 and R7, Fig. 3) are predicted to contain turns (Fig. 2) that are likely to be on the molecular surface and available for interaction.

Binding Site for $G_{\beta\gamma}$. Partial digestion experiments show that loss of the N terminus is correlated with loss of ability to bind $G_{\beta\gamma}$, and that $G_{\beta\gamma}$ binding to this region blocks cleavage (24–27). This argues that this region is the site of $G_{\beta\gamma}$ binding. Although there is substantial sequence variation (Fig. 1) in the N-terminal region, its secondary structure is consistently predicted as α -helical (Fig. 2). This may not be the only site of interaction, since ADP-ribosylation by cholera toxin at residue 179 has been shown to reduce the binding affinity between the G_α and $G_{\beta\gamma}$ (34). According to our model both the N terminus and cholera toxin modification site are on the “membrane” side of the molecule (Fig. 3).

Binding Site of the Receptor Protein. Several lines of evidence point to the C-terminal region of G_α as the site of receptor interaction. (i) ADP-ribosylation of Cys-352 by pertussis toxin has been observed to block interaction of $G_{\alpha i}$ with photorhodopsin (33). (ii) A mutant of G_{as} that cannot be activated by hormone receptors has been shown to be due to replacement of arginine in the C-terminal region (residue 350 of the G_α consensus) by proline (28). Also, competition

studies indicate that synthetic peptides corresponding to G_{α} residues 316–334 and residues 345–355 compete with $G_{\alpha t}$ for interaction with rhodopsin and that, in the first peptide, replacement of Cys-326 completely blocks this competition (32). Finally, a chimeric $G_{\alpha i}/G_{\alpha s}$ hybrid (31) composed of the N-terminal 60% of $G_{\alpha i}$ and the C-terminal 40% of $G_{\alpha s}$ mediates stimulation of the $G_{\alpha s}$ receptor as well as the normal $G_{\alpha s}$ polypeptide.

Thus, all studies to date indicate that the C-terminal region past residue 315 contains the receptor-binding site. The relatively high sequence conservation among G proteins in this region may account for observed cross-reactivity of G proteins with their receptors. In the three-dimensional structure of $p21^{ras}$, the C-terminal region is in physical proximity to the N-terminal region on the same (membrane) side of the molecule (1). Similarly, our proposed three-dimensional model of G_{α} indicates that the C-terminal region, proposed to be the receptor-binding site, is spatially close to the N-terminal region proposed for $G_{\beta\gamma}$ binding. This suggests the possibility of quaternary interaction among $G_{\beta\gamma}$, G_{α} , and the receptor protein.

SUMMARY

We propose a model for the structure of G_{α} based on the crystal structure of the catalytic fragment of the functionally similar HRAS protein. The sequence similarity within regions important for structure and function leads to the conclusion that the architecture of the G_{α} core is the same as that of $p21^{ras}$ and that differences accounting for the specific properties of the proteins occur in regions that link the core elements.

Our model contains a number of specific differences and findings compared with earlier models based on the structure of G-EF-Tu (6, 7). Some of the differences are (i) topology of the β -strands in the N-terminal half of the molecule, (ii) attachment site of the Mg^{2+} involved in phosphate binding and hydrolysis (L1 of our model as opposed to L4 in G-EF-Tu), and (iii) division of G_{α} consensus residues 64–196 into two domains R2 and R3 in our model, compared to only one insertion in the G-EF-Tu model. Findings from our model include (i) orientation of the G_{α} model with respect to the membrane (possible since the orientation of $p21^{ras}$ with respect to the membrane is implied by its structure); (ii) identification of residues corresponding to 30 and 117 of $p21^{ras}$ as ligands of the ribose of guanosine; (iii) alignment of the C-terminal region of G_{α} consensus with that of $p21^{ras}$, thus allowing the conclusion that the C-terminal and N-terminal regions are in spatial proximity; (iv) assignment of the $G_{\beta\gamma}$ interaction site to the N terminus and the receptor interaction site to the C-terminal region of G_{α} , both on the membrane face of the protein and in close enough proximity for interaction; (v) location of the GDP binding site on the cytoplasmic face of G_{α} by analogy to the $p21^{ras}$ structure; and (vi) assignment of the sites of cholera and pertussis toxin modification on the membrane face of G_{α} , consistent with their biological effects on $G_{\beta\gamma}$ and receptor interaction.

The location of the effector binding site is still an open question. Current experimental data suggest either the R6 (membrane face) or R7 loop (cytoplasmic face) as the site of effector interaction, whereas the large R2 domain is analogous to the region proposed for effector interaction in $p21^{ras}$. Only future experimental studies will clarify these points. We hope that this model will stimulate such studies into the structure of G proteins and thereby be self-improving.

The authors are grateful to Michael Matsko, Liang Tong, and Bart de Vos for their assistance. We also thank Susan Masters and Henry Bourne for preprints of their work and valuable discussions. We acknowledge the support of the Office of Energy Research Health Effects Research in Biological Systems Division of the U.S. Department of Energy (contract DE-AC03-76SF000098) and a National Institutes of Health grant (CA 45593).

- de Vos, A. M., Tong, L., Milburn, M. V., Matias, P. M., Jancarik, J., Noguchi, S., Nishimura, S., Miura, K., Ohtsuka, E. & Kim, S.-H. (1988) *Science* **239**, 888–893.
- Stryer, L. & Bourne, H. R. (1986) *Annu. Rev. Cell. Biol.* **2**, 391–419.
- Gilman, A. G. (1987) *Annu. Rev. Biochem.* **56**, 615–649.
- Cassey, P. J. & Gilman, A. G. (1988) *J. Biol. Chem.* **263**, 2577–2580.
- Neer, E. J. & Clapham, D. E. (1988) *Nature (London)* **333**, 129–134.
- Masters, S. B., Stroud, R. M. & Bourne, H. R. (1986) *Protein Eng.* **1**, 47–54.
- Deretic, D. & Hamm, H. E. (1987) *J. Biol. Chem.* **262**, 10839–10847.
- Hingorani, V. N. & Ho, Y.-K. (1987) *FEBS Lett.* **220**, 15–22.
- Jurjak, F. (1985) *Science* **230**, 32–36.
- LaCour, T. F. M., Nyborg, J., Thirup, S. & Clark, B. F. C. (1985) *EMBO J.* **4**, 2385–2388.
- Moller, W. & Amons, R. (1985) *FEBS Lett.* **186**, 1–7.
- Kim, S.-H., de Vos, A. M., Tong, L., Milburn, M. V., Matias, P. M., Jancarik, J. & Nishimura, S. (1988) *Cold Spring Harbor Symp. Quant. Biol.* **53**, in press.
- Barbacid, M. (1987) *Annu. Rev. Biochem.* **56**, 779–827.
- Tanabe, T., Nukada, T., Nishikawa, Y., Sugimoto, K., Suzuki, H., Takahashi, H., Noda, M., Haga, T., Ichihara, A., Kangawa, K., Minamino, N., Matsuo, H. & Numa, S. (1985) *Nature (London)* **315**, 242–245.
- Lochrie, M. A., Hurley, J. B. & Simon, M. I. (1985) *Science* **228**, 96–99.
- Jones, D. T. & Reed, R. R. (1987) *J. Biol. Chem.* **262**, 14241–14249.
- Sobel, E. & Martinez, H. M. (1986) *Nucleic Acids Res.* **14**, 363–374.
- Rose, G. D., Gaselowitz, A. R., Lesser, G. J., Lee, R. H. & Zehfus, M. H. (1985) *Science* **229**, 834–838.
- Finer-Moore, J. & Stroud, R. M. (1984) *Proc. Natl. Acad. Sci. USA* **81**, 155–159.
- Feng, D. F., Johnson, M. S. & Doolittle, R. F. (1985) *J. Mol. Evol.* **21**, 112–125.
- Chou, P. Y. & Fasman, G. D. (1978) *Annu. Rev. Biochem.* **47**, 251–276.
- Lesk, A. M., Levitt, M. & Chothia, C. (1986) *Protein Eng.* **1**, 77–78.
- Barton, G. J. & Sternberg, M. J. E. (1987) *Protein Eng.* **1**, 89–94.
- Hurley, J. B., Simon, M. I., Teplow, D. B., Robishaw, J. D. & Gilman, A. G. (1984) *Science* **226**, 860–862.
- Neer, E. J., Pulsifer, L. & Wolf, L. G. (1988) *J. Biol. Chem.* **263**, 8996–9000.
- Fung, B. K.-K. & Nash, C. R. (1983) *J. Biol. Chem.* **258**, 10503–10510.
- Navon, S. E. & Fung, B. K.-K. (1987) *J. Biol. Chem.* **262**, 15746–15751.
- Sullivan, K. A., Miller, R. T., Masters, S. B., Beiderman, B., Heideman, W. & Bourne, H. R. (1987) *Nature (London)* **330**, 758–760.
- Miller, R. T., Masters, S. B., Sullivan, K. A., Beiderman, B. & Bourne, H. R. (1988) *Nature (London)* **334**, 712–715.
- Bourne, H. R., Masters, S. B., Miller, R. T., Sullivan, K. A. & Heideman, W. (1988) *Cold Spring Harbor Symp. Quant. Biol.* **53**, in press.
- Masters, S. B., Sullivan, K. A., Miller, R. T., Beiderman, B., Lopez, N. G., Ramachandran, J. & Bourne, H. R. (1988) *Science* **241**, 448–451.
- Hamm, H. E., Deretic, D., Arendt, A., Hargrave, P. A., Koenig, B. & Hofmann, K. P. (1988) *Science* **241**, 832–835.
- Van Dop, C., Yamanaka, G., Steinberg, F., Sekura, R. D., Manclark, C. R., Stryer, L. & Bourne, H. R. (1984) *J. Biol. Chem.* **259**, 23–26.
- Kahn, R. A. & Gilman, A. G. (1984) *J. Biol. Chem.* **259**, 6235–6240.
- Sigal, I. S., Gibbs, J. B., D'Alonzo, J. S. & Scolnick, E. M. (1986) *Proc. Natl. Acad. Sci. USA* **83**, 4725–4729.
- Cales, C., Hancock, J. F., Marshall, C. J. & Hall, A. (1988) *Nature (London)* **332**, 548–551.
- Adari, H., Lowy, D. R., Willumsen, B. M., Der, C. J. & McCormick, F. (1988) *Science* **240**, 518–521.